



Solute Spreading in Variably Saturated Spatially Heterogeneous Formations: The Role of Water Saturation and Soil Texture

David Russo

Institute of Soil, Water and Environmental Sciences, Agricultural Research Organization,
The Volcani Center, POB 6, Bet Dagan 50250, Israel

Email: vwrosd@agri.gov.il



1. Background

Solute transport in near-surface geological formations is considerably affected by the heterogeneity in the hydraulic properties (HP) of the formations. The latter may be characterized by a relatively complex correlation structure. In the approach adopted here, the spatial arrangement of distinct geological materials (e.g., sand or clay deposits) is replaced by a single, composite material whose properties are bimodal and statistically homogeneous. The composite heterogeneous formation, in turn, is viewed as a mixture of two populations (background soil and embedded soil) of differing spatial structures.

2. Purpose of the Presentation

- To employ first-order, Lagrangian-stochastic framework of vadose zone transport in order to investigate the combined effect of the embedded soil's texture and the mean pressure head (i.e., water saturation) on solute spread and breakthrough in a composite, bimodal, heterogeneous, variably saturated formations, and,
- To test the applicability of the results of the first-order analyses (FOA) to more realistic conditions.

3. Theoretical Considerations

Consider the vadose zone of the composite formation. The mean flow takes place normal to its strata. The composite formation is variably saturated and its flow parameters depend on water saturation in a manner which is highly dependent on the texture of the two distinct soil materials that assemble the formation. It is assumed here that the constitutive relationships for unsaturated flow for the i -th soil material of the composite formation are given by the 2-parameter *Gardner-Russo* model, i.e., K_{si} and α_i , $i=1,2$. Quantification of the vadose-zone transport is based on a two-stage approach which combines:

- a first-order perturbation approximation of the 3-D steady-state unsaturated flow equation; and
- a general Lagrangian description of the motion of an indivisible particle of a passive solute carried by a steady-state flow.

Literature Cited

Russo, D., 2004. Stochastic analysis of macrodispersion in heterogeneous bimodal variably saturated formations: The effect of water saturation. *Water Resour. Res.* 40: W09201, doi:10.1029/2004WR003045.
Russo, D., 2010. First-order and numerical analyses of flow and transport in heterogeneous, bimodal variably saturated formations. *Water Resour. Res.* 46, W06509, doi:10.1029/2009WR008307.

4. Results - First Order Analyses

Results of the FOA (Russo, 2004; 2010) suggest that in variably saturated, bimodal heterogeneous formations, $\log K$ variance, σ_y^2 , is a concave function of the mean pressure head, $H=E[\psi(\mathbf{x})]$. The concave nature of the $\sigma_y^2(H)$ relationships stems from the basic differences between the local K - ψ relationships associated with coarse-textured soils and their counterparts associated with fine-textured soils. Consequently, the magnitude of the principal components of the time-dependent macrodispersion tensor (Fig. 1) are also concave functions of H .

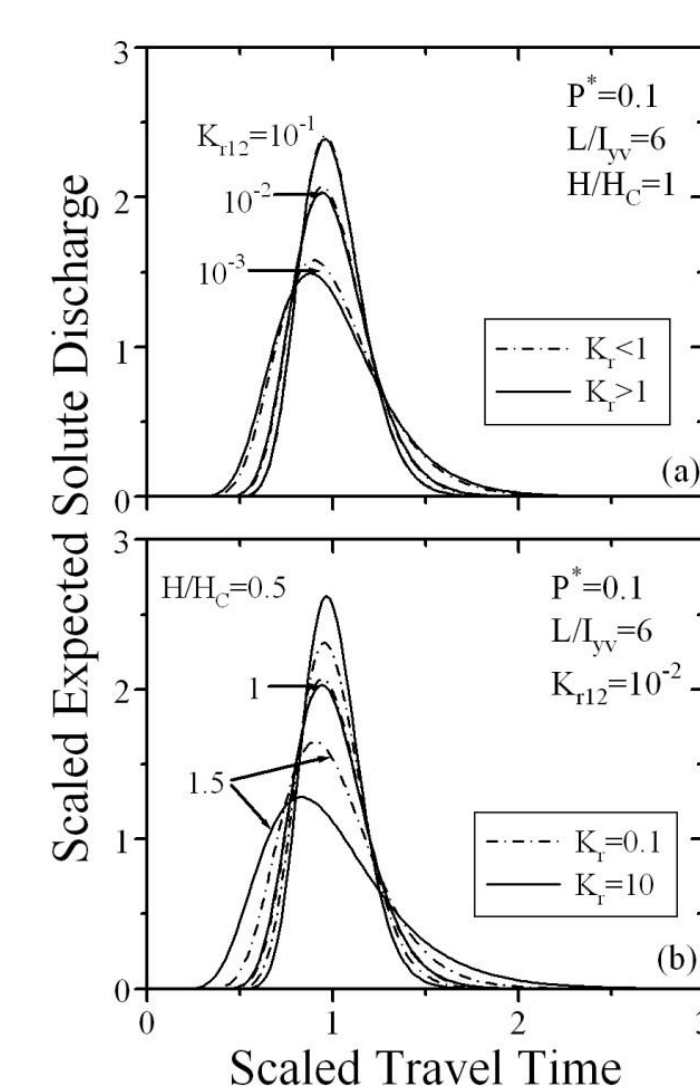
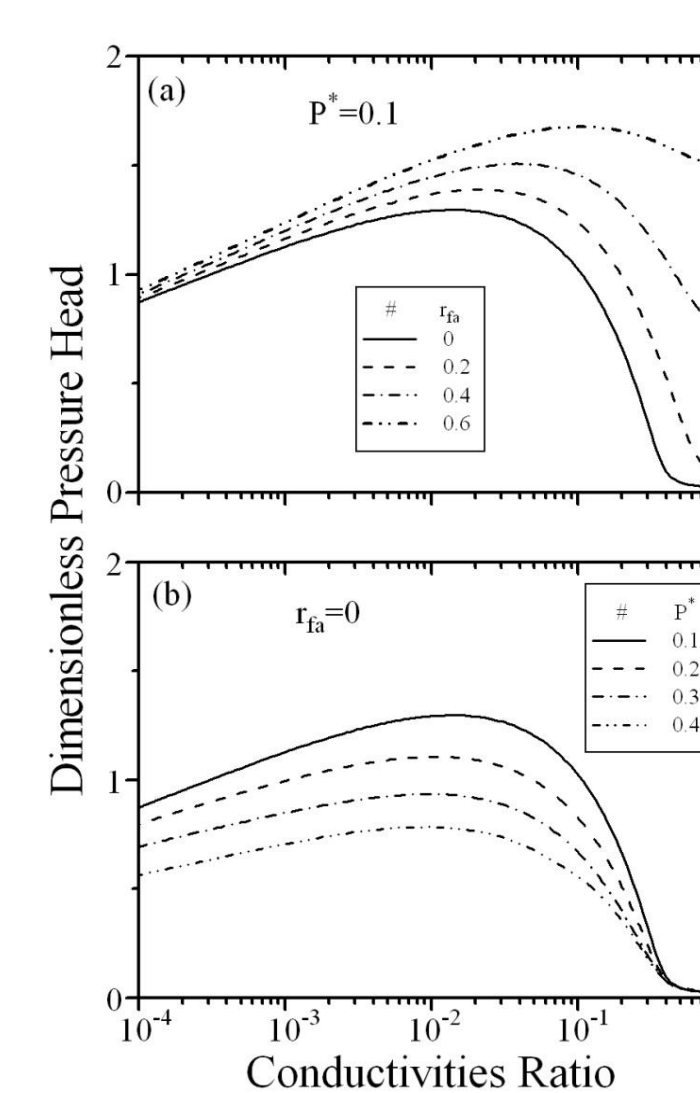
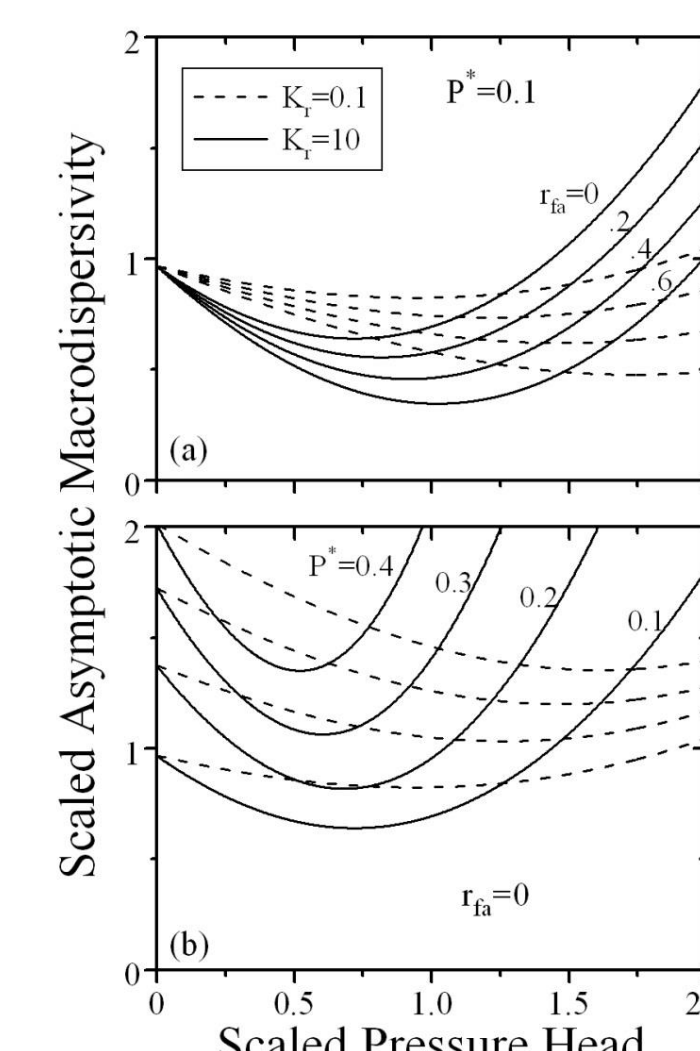
Figure 1: Scaled longitudinal asymptotic macrodispersivity, $D^*=D^*_{11}/U_1\lambda_{yv1}$, as a function of the scaled H , $H^*=\Gamma_1 H$, for fine- ($K_r < 1$, case 1) and coarse- ($K_r > 1$, case 2) textured embedded soils. P^* is the embedded soil volume fraction, $\Gamma_1 = \exp(E[A_1])$ and r_{fa} is the cross-correlation coefficient.

Fig. 1 suggests that at intermediate values of H^* , a crossover occurs between values of D^* associated with the two cases. Values of H^* at which crossover occurs, H^*_C , are depicted in Fig. 2.

Figure 2: Dimensionless mean pressure head H^*_C at which D^* associated with the two cases are identical, as a function of the ratio, $K_{r12}=K_{r1}/K_{r2}$.

The dependence of both D^* and solute mass flux on the velocity field statistics, implies that the value of H^*_C may be used to identify crossover behavior of the expected solute BTCs associated with the two cases (Fig. 3).

Figure 3: Scaled expected solute discharge, $SL/U_1 M_0$, crossing a horizontal CP located at a given scaled vertical distance, L/λ_{yv1} from the injection zone, as a function of the scaled travel time, $t'=tU_1/L$, for the two cases.



5. Numerical Simulations

The stringent assumptions of the FOA may oversimplify the processes occurring in realistic variably saturated flow systems. The applicability of the results presented here to more realistic situations, is briefly analyzed. A series of numerical analyses of flow and transport in a hypothetical, yet realistic, 3-D variably saturated heterogeneous, bimodal formations were conducted (Russo, 2010). Two different flow regimes were considered. The first is a relatively simple, steady-state (SS) flow, pertinent to the flow conditions assumed in the FOA. The second is a transient (TR) flow, pertinent to realistic situations involving periodic forcing conditions at the soil surface and water uptake by plant roots.

Mean, Y , and variance, σ_y^2 , of $\log K$ evaluated from a series of SS simulations for values of imposed pressure head, ψ_0 (Fig. 4), clearly exhibit crossover behavior.

Figure 4: Y (a) and σ_y^2 (b) as functions of the imposed pressure head ψ_0 .

Furthermore, the pressure head SD, σ_ψ , and the fraction, F_{em} , of embedded soil volume associated with K values that exceed those of the background soil, (Fig. 5) also exhibit crossover behavior.

Figure 5: σ_ψ , (a) and F_{em} (b), as functions of the imposed pressure head, ψ_0 .

6. Conclusions

In SS flows, features of transport associated with the two different formations exhibit a crossover behavior at intermediate water saturations. This explains why in TR flows associated with active root zone, the response of the different formations is essentially independent of the texture of the embedded soil.

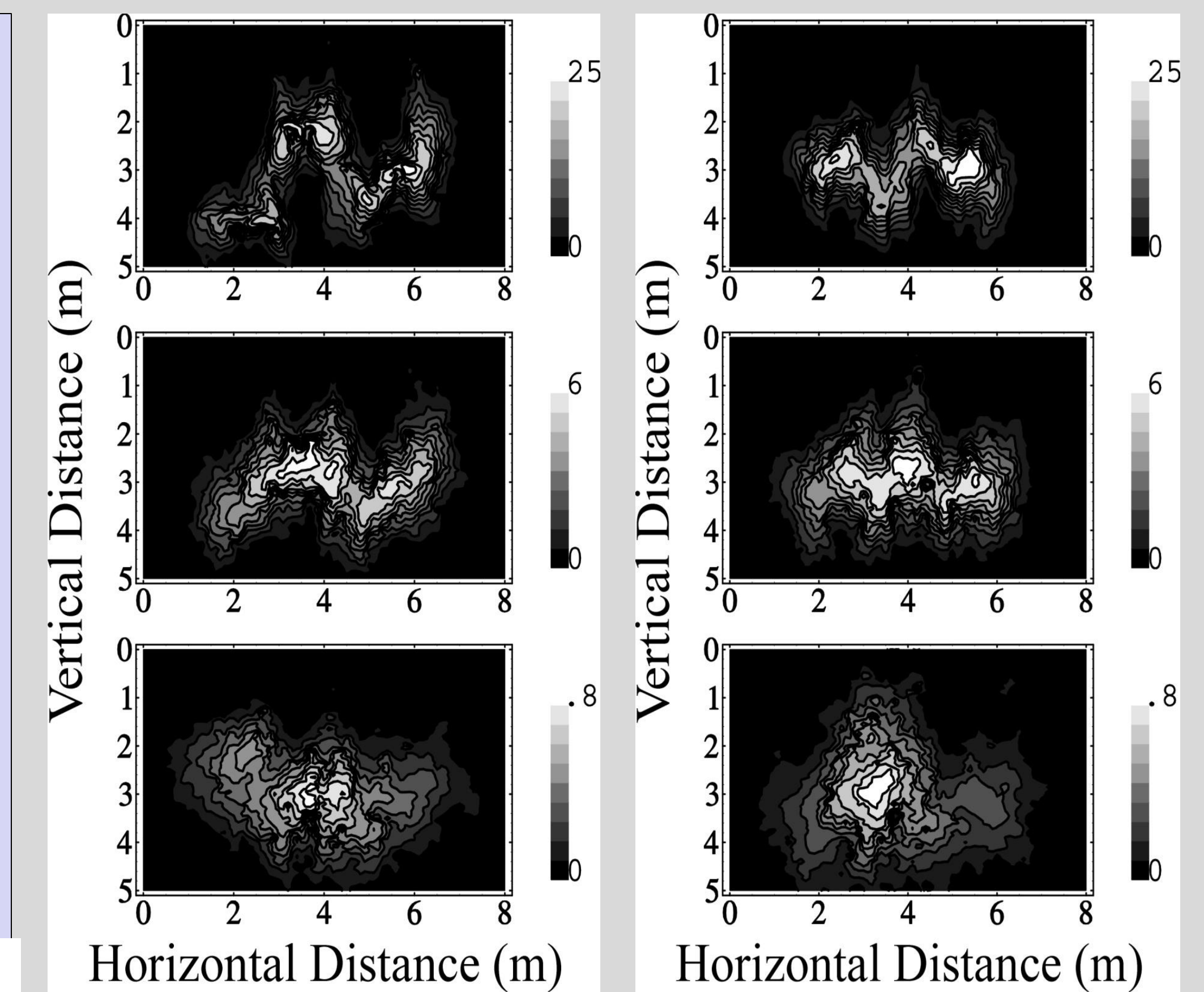


Figure 6: SS flows: contours of concentrations in a vertical x_1x_2 -plane of the flow system at $x_3=4m$, for case 1 (left) and case 2 (right), for 3 different values of ψ_0 , -0.8m (a), -1.6m (b) and -5m (c).

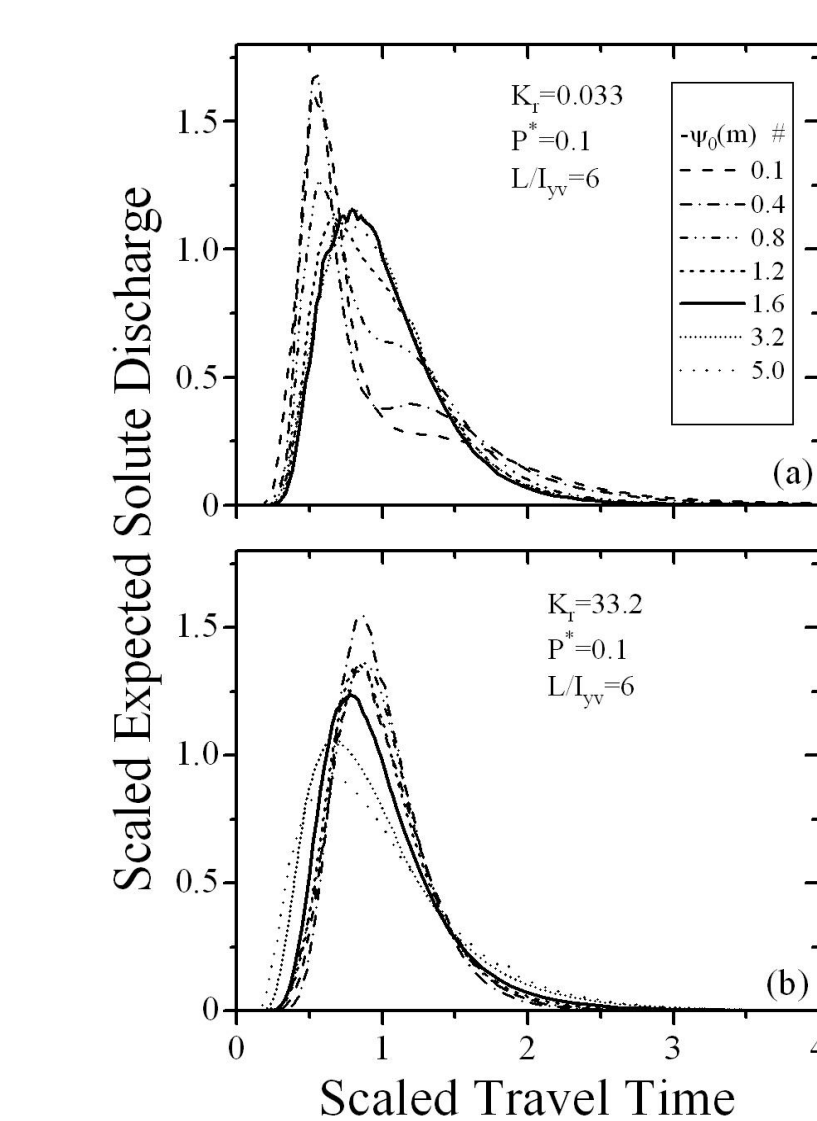


Figure 7: SS flows: scaled expected solute BTC at a CP located at $L=1.2m$, for the 1st (a) and the 2nd (b) cases and for selected values of ψ_0 .

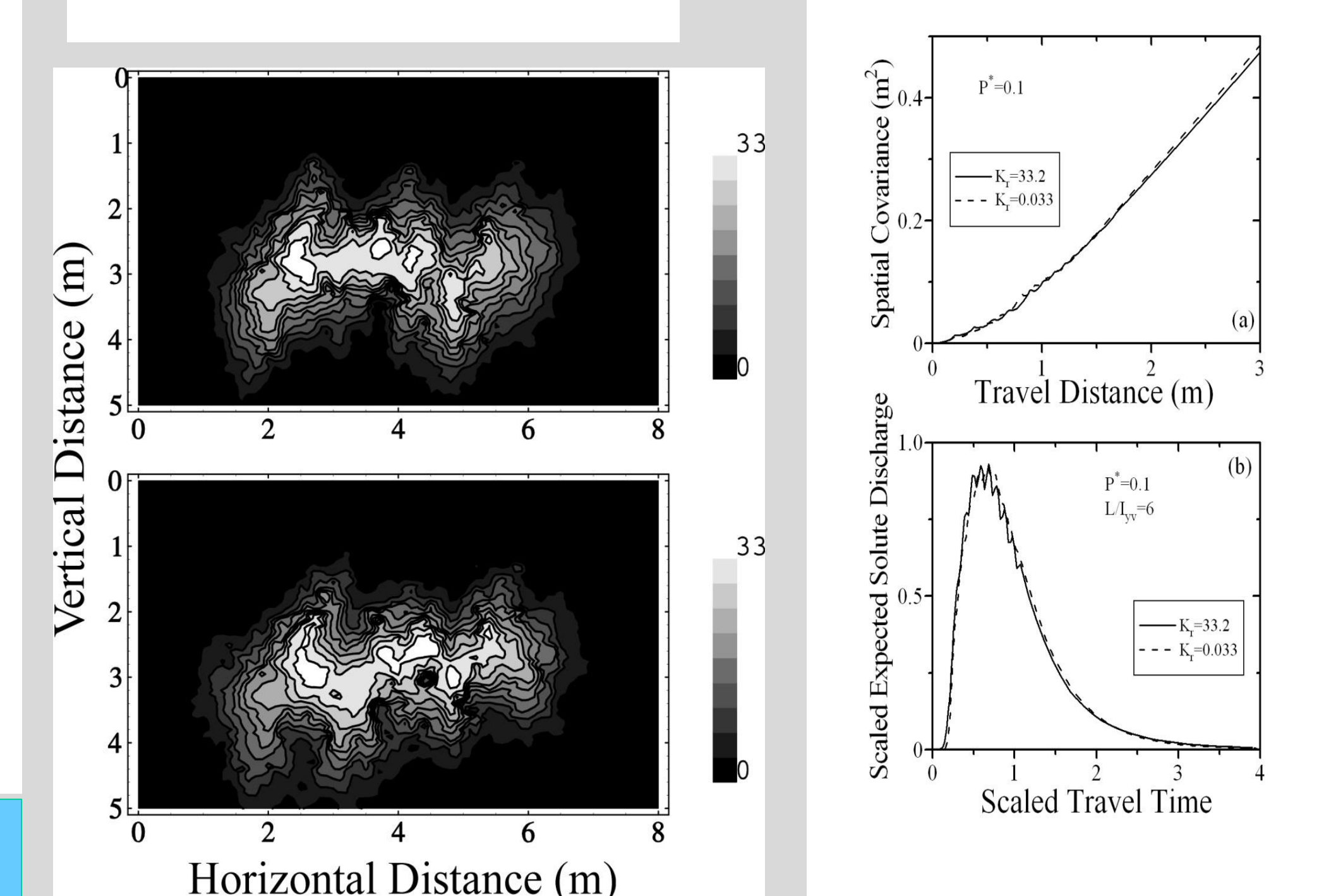


Figure 8: TR flows: left: contours of concentrations in a vertical x_1x_2 -plane of the flow system at $x_3=4m$, for case 1 (up) and case 2 (bottom). Right: longitudinal component of the spatial covariance tensor (a), and the scaled expected solute BTC at a CP located at $L=1.2m$ (b).